

Persistent Corner Spin Mode at the Quantum Critical Point of a Plaquette Heisenberg Model

Yining Xu,¹ Zijian Xiong,^{2,3,*} and Long Zhang^{4,†}

¹*College of Physics and Electronic Engineering, Chongqing Normal University, Chongqing 401331, China*

²*Department of Physics, and Center of Quantum Materials and Devices, Chongqing University, Chongqing, 401331, China*

³*Chongqing Key Laboratory for Strongly Coupled Physics, Chongqing, 401331, China*

⁴*Kavli Institute for Theoretical Sciences and CAS Center for Excellence in Topological Quantum Computation, University of Chinese Academy of Sciences, Beijing 100190, China*

The fate of the gapless or degenerate edge modes of topological states at the bulk quantum critical points (QCPs) has triggered intensive research recently. In this work, we numerically study the critical behavior of the corner states at the QCP of a plaquette Heisenberg model with open boundary condition, which in the disorder phase hosts both a dangling corner state with a symmetry-protected spin-1/2 mode as a hallmark of the higher-order topological phase, and nondangling corners. We show that the dangling spin mode induces a new universality class of the corner critical behavior, which is distinct from the ordinary case of the nondangling corner. In particular, we show that the degenerate spin mode persists at the QCP despite its coupling to the critical spin fluctuations in the bulk. This shows the unexpected robustness of the corner mode of the higher-order topological phase.

I. INTRODUCTION

Phase transitions and critical phenomena are among the central topics of condensed matter and statistical physics. The canonical understanding of continuous phase transitions, the Landau-Ginzburg-Wilson (LGW) theory¹, has been developed since the 1940s based on the notions of spontaneous symmetry breaking and the renormalization group (RG) transformations. Most of classical critical points and a large part of quantum critical points (QCPs) belong to the Wilson-Fisher universality classes, which only depend on the broken symmetry at the phase transition and the space (or spacetime) dimensionality. Quantum phase transitions beyond the LGW paradigm, such as the deconfined quantum critical point (DQCP)^{2,3}, are under intensive research, in which the quantum Berry phases and topological terms play a prominent role⁴⁻⁶.

A d -dimensional critical system with a $(d - 1)$ -dimensional boundary shows rich surface critical behavior, which is controlled by the interactions near the boundary. The surface criticality of the classical phase transitions has been well-documented in the literature^{7,8}, which can be classified based on whether the boundary has a long-range order at the bulk critical point. In the ordinary class, the surface remains disordered throughout the disorder phase in the bulk, and the surface critical behavior is fully induced by the divergent correlation length in the bulk. If the surface interaction is so strong that it develops a long-range order at a higher temperature than the bulk, the surface exhibits additional critical behavior at the bulk transition, which is classified as the extraordinary transition. Fine-tuning the surface interaction can lead to a special transition, where the surface and the bulk ordering transitions merge at the same temperature.

The interest in the surface critical behavior particularly as QCPs has revived recently in order to unveil the fate of the gapless or degenerate surface modes of topological states as the bulk undergoes quantum phase transitions (QPTs). It is shown that in certain models of topological superconductors the Majorana edge modes are robust against the critical quantum fluctuations in the bulk⁹⁻¹². In the two-dimensional (2D) Affleck-Kennedy-Lieb-Tasaki (AKLT) model, the gapless edge state changes the universality class of the surface critical behavior of the (2+1)D O(3) Wilson-Fisher QCP¹³. This new surface universality class is also realized in similar models with dangling spin chains on the edge¹⁴⁻¹⁷ and has triggered further theoretical studies¹⁸⁻²⁶.

The notion of symmetry-protected topological (SPT) states has been generalized into the higher-order (HO) topological states with lower-dimensional edge modes²⁷⁻³⁵. A simple example is provided by the spin-1/2 antiferromagnetic Heisenberg model on a plaquette-modulated square lattice, which is shown in Fig. 1. For $J_2/J_1 \ll 1$, all spins in the bulk form plaquette singlets thus the bulk is in a gapped disorder state. With the open boundary condition, the dimerized edge is also gapped, but corner A in Fig. 1 hosts a dangling spin-1/2 mode, whose degeneracy is protected by the spin rotation and the lattice C_4 rotation and the R_{xy} reflection symmetries³⁴⁻³⁶. Therefore, this plaquette Heisenberg model realizes a second-order SPT state with a degenerate corner mode. The HOSPT phase and the lower-dimensional boundary mode can be captured by a topological term in the effective field theory^{34,36}. Tuning the interaction J_2/J_1 induces a QPT from the disorder phase to an antiferromagnetic order in the $J_2/J_1 \simeq 1$ regime, which belongs to the (2+1)D O(3) universality class³⁷⁻⁴⁰. The direct topological QPT between different disorder phases is also studied recently³⁶.

In this work, we study the critical behavior of the cor-

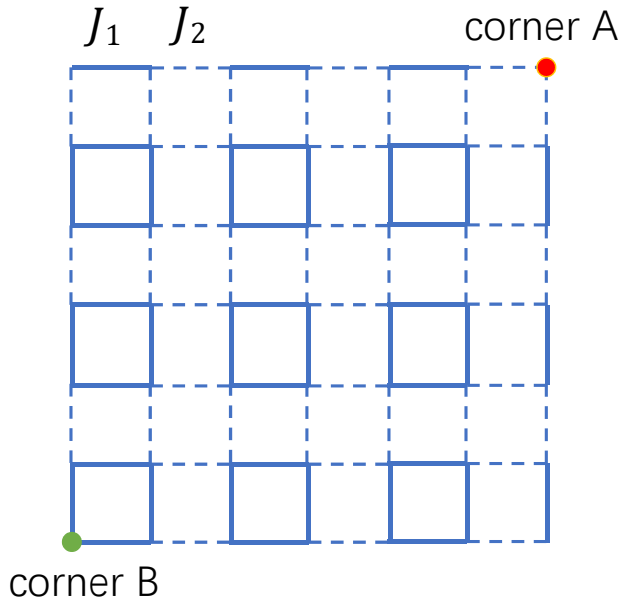


FIG. 1. Structures of the plaquette square lattice. Each unit cell (a plaquette) is composed of four sites. The intra-unit-cell interaction J_1 and the inter-unit-cell interaction J_2 are represented by solid and dashed bonds, respectively. There is a dangling spin at corner A with a degenerate spin-1/2 mode in the $J_2/J_1 \ll 1$ regime, while corner B is called the nondangling corner.

ner state at the bulk QCP between the disorder and the antiferromagnetic order phases, and focus on the difference of the corner states with or without a dangling spin. With quantum Monte Carlo simulations on lattices with open boundary condition, we find such two corner states exhibit distinct critical behavior with different critical exponents. In particular, we find that the degenerate spin-1/2 mode at the dangling corner persists at the QCP despite its coupling to the critical spin fluctuations in the bulk, which is reminiscent of the extraordinary class of the classical surface critical behavior.

The paper is organized as follows: In Sec. II, we introduce the model and the spin correlation functions used to characterize the corner critical behavior. In Sec. III, the correlation functions of the dangling and the nondangling corner spins are presented, from which the critical exponents are extracted. A summary is given in Sec. IV.

II. MODEL AND METHODS

We study the $S = 1/2$ antiferromagnetic Heisenberg model on the plaquette square lattice shown in Fig.1. Each unit cell (a plaquette) is composed of four sites.

The Hamiltonian is given by

$$H = J_1 \sum_{\langle i,j \rangle} \mathbf{S}_i \cdot \mathbf{S}_j + J_2 \sum_{\langle i,j \rangle'} \mathbf{S}_i \cdot \mathbf{S}_j, \quad (1)$$

where J_1 and J_2 are the nearest-neighbor antiferromagnetic Heisenberg interactions of intra- and inter-unit-cell bonds, respectively. In the $J_2/J_1 \ll 1$ limit, each plaquette forms a spin singlet state at the ground state, thus the system is in a gapped disorder phase, which is called the plaquette valence bond solid (PVBS) phase. For $J_2/J_1 \simeq 1$, the system has a long-range Néel order. There is a quantum phase transition from the PVBS phase to the Néel order at $J_2/J_1 = 0.548524$, which belongs to the 3D $O(3)$ universality class^{37–40}. In this work, we set $J_1 = 1$.

It is realized recently that this plaquette Heisenberg model is an example of HOSPT phase^{34–36}. In the disorder phase, as shown in Fig. 1, the lattice with open boundary has a dangling spin 1/2 at corner A, because all strong bonds connecting to the corner site are cut. This dangling spin 1/2 forms a degenerate corner mode, which is protected by the spin rotation symmetry together with the crystal symmetry: the plaquette-centered C_4 rotation and the diagonal reflection R_{xy} symmetry. On the other hand, the spin on corner B forms a singlet with its neighboring sites, and is not degenerate.

In this work, we use the stochastic series expansion (SSE) quantum Monte Carlo (QMC) simulations^{41–44} to study the corner critical behavior of the plaquette Heisenberg model with open boundary. The lattice size is $L \times L$ with $33 \leq L \leq 81$. The inverse temperature $\beta = L$. All simulations are performed at the bulk quantum critical point (QCP) $J_2/J_1 = 0.548524$.

The following spin correlation functions and the corresponding anomalous dimensions are introduced to characterize the critical behavior of the corner spin at the QCP: the equal-time correlation of the corner spin (with subscript c) at $(0,0)$ and a bulk spin (with subscript b) at (r,r) ,

$$C_{cb}(r) = \langle S_r^z S_0^z \rangle \propto r^{-(d+z-2+\eta_{cb})}, \quad (2)$$

and the equal-time correlation of the corner spin at $(0,0)$ and a spin on the edge (with subscript s) at $(r,0)$,

$$C_{cs}(r) = \langle S_r^z S_0^z \rangle \propto r^{-(d+z-2+\eta_{cs})}, \quad (3)$$

and the imaginary-time correlation of the spin at the corner,

$$C_{cc}(\tau) = \langle S^z(\tau) S^z(0) \rangle \propto \tau^{-(d+z-2+\eta_{cc})/z}. \quad (4)$$

Here, $d = 2$ is the spatial dimension, and $z = 1$ is the dynamical exponent of the QCP.

These anomalous dimensions can be derived from the scaling dimensions of the spin operators in the bulk, on the edge and at the corner, which are denoted by Δ_b , Δ_s

TABLE I. Anomalous dimensions of the corner critical behavior for both the nondangling and the dangling corner spins.

	η_{cb}	η_{cs}	η_{cc}	Δ_c
Nondangling	1.24(6)	1.78(8)	2.34(3)	1.67(2)
Dangling	0.33(3)	1.06(3)	0.682(11)	0.84(1)

and Δ_c , respectively:

$$d + z - 2 + \eta_{cb} = \Delta_c + \Delta_b, \quad (5)$$

$$d + z - 2 + \eta_{cs} = \Delta_c + \Delta_s, \quad (6)$$

$$d + z - 2 + \eta_{cc} = 2\Delta_c. \quad (7)$$

Moreover, the anomalous dimensions in the bulk η and on the edge η_{\parallel} are defined by

$$d + z - 2 + \eta = 2\Delta_b, \quad (8)$$

$$d + z - 2 + \eta_{\parallel} = 2\Delta_s, \quad (9)$$

thus we have the following scaling relations,

$$2\eta_{cb} = \eta + \eta_{cc}, \quad (10)$$

$$2\eta_{cs} = \eta_{\parallel} + \eta_{cc}. \quad (11)$$

These relations will serve as consistency check to the numerical results. For the 3D O(3) universality class $\eta = 0.0386(12)^{45,46}$. The edge is always gapped in the paramagnetic phase, thus the surface critical behavior belongs to the ordinary class with $\eta_{\parallel} = 1.338^{47-49}$.

The spatial correlations $C_{cb}(r)$ and $C_{cs}(r)$ show even-odd effect as a function of the distance r due to the plaquette modulation. Therefore, we fit the correlation functions of a given lattice size L for even and odd distances r separately to extract the anomalous dimensions $\eta_i^e(L)$ and $\eta_i^o(L)$ ($i = cb$ or cs). We then extrapolate to the thermodynamic limit with the following scaling form,

$$\eta_i^{e/o}(L) = \eta_i^{e/o} + cL^{-\omega}. \quad (12)$$

III. NUMERICAL RESULTS

A. Nondangling corner

We first study the critical behavior of the nondangling corner (corner B in Fig. 1), which is dubbed the ordinary transition of the corner criticality, because the corner spin is gapped in the disorder phase. The correlation functions $C_{cb}(r)$ and $C_{cs}(r)$ are shown in Fig. 2. Using the finite-size scaling analysis introduced in Sec. II, we find the following anomalous dimensions for $C_{cb}(r)$, $\eta_{cb}^e = 1.23(6)$, and $\eta_{cb}^o = 1.26(4)$, which are consistent with each other within error bars. Our final estimate is

$$\eta_{cb} = 1.24(6). \quad (13)$$

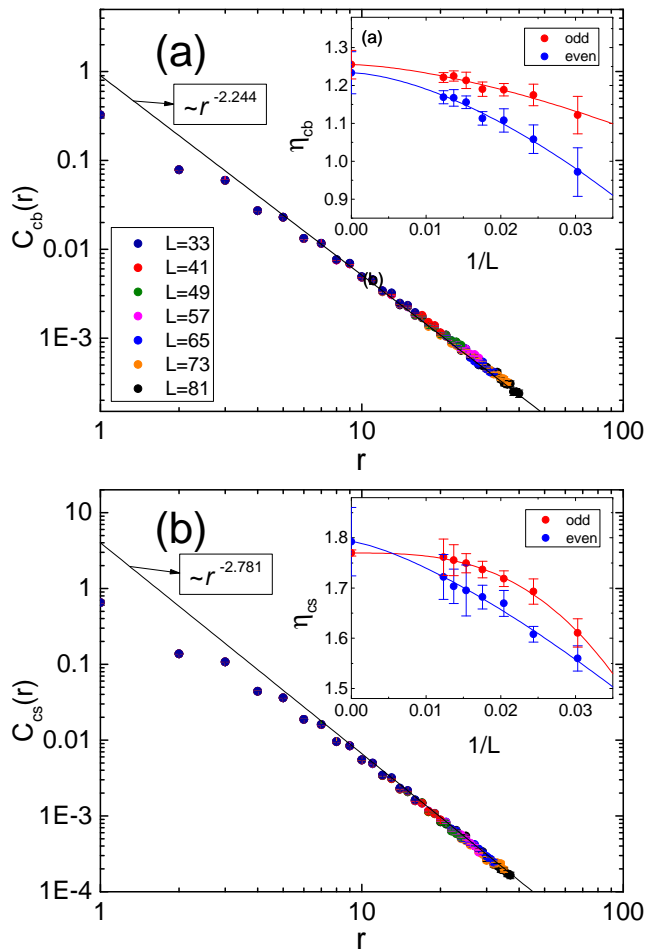


FIG. 2. Spatial correlation functions (a) $C_{cb}(r)$ and (b) $C_{cs}(r)$ of the nondangling corner spin. The black lines are the reference for the power-law decay with the extrapolated critical exponents, $\eta_{cb} = 1.24(6)$ and $\eta_{cs} = 1.78(8)$. Insets: the finite-size scaling of the critical exponents η_{cb} and η_{cs} with Eq. (12).

With similar analysis, we find for $C_{cs}(r)$, $\eta_{cs}^e = 1.79(7)$, and $\eta_{cs}^o = 1.77(1)$, and our final estimate is

$$\eta_{cs} = 1.78(8). \quad (14)$$

The imaginary time correlation function of the corner spin $C_{cc}(\tau)$ is shown in Fig. 3. Fitting to Eq. (4) and then Eq. (12), we find the anomalous dimension

$$\eta_{cc} = 2.34(3). \quad (15)$$

These anomalous dimensions are listed in Table I. The scaling relations in Eq. (10) and (11) are respected within error bars. Therefore, our final estimate of the scaling dimension of the corner spin operator at the ordinary transition is

$$\Delta_c = 1.67(2). \quad (16)$$

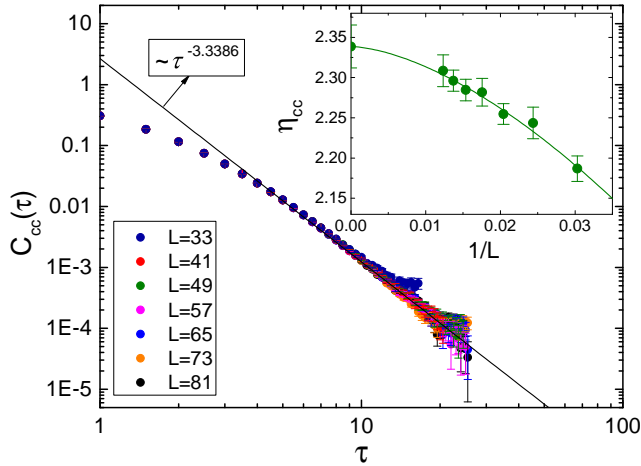


FIG. 3. Imaginary-time correlation function $C_{cc}(\tau)$ of the nondangling corner spin. The black line is the reference for the power-law decay with the extrapolated critical exponent, $\eta_{cc} = 2.34(3)$. Inset: the finite-size scaling of the critical exponent η_{cc} with Eq. (12).

B. Dangling corner

The dangling corner has a degenerate spin-1/2 mode in the bulk disorder phase, which spontaneously breaks the spin rotational symmetry at the corner. This is similar to the extraordinary class of classical surface critical behavior with a long-range order on the surface in the bulk disorder phase. We hence expect that it leads to corner critical behavior distinct from the ordinary class. The spatial correlation functions $C_{cb}(r)$ and $C_{cs}(r)$, and the imaginary-time correlation $C_{cc}(\tau)$ are shown in Figs. 4 and 5, respectively.

We first note that $C_{cc}(\tau)$ does not decay to zero as τ grows, indicating a persistent spin mode at the corner despite its coupling to the critical bulk state. We thus include a constant term in the fitting,

$$C_{cc}(\tau) = m_c^2 + b\tau^{-1-\eta_{cc}}. \quad (17)$$

The anomalous dimension η_{cc} obtained from different lattice sizes is then extrapolated to the thermodynamic limit with Eq. (12). The result is

$$\eta_{cc} = 0.682(11). \quad (18)$$

The constant term in Eq. (17) indicates a free local moment at the corner, which can be extrapolated with

$$m_c^2(L) = m_c^2 + bL^{-\omega}, \quad (19)$$

and we find

$$m_c^2 = 0.3896(5) \quad (20)$$

Therefore, we may dub the corner critical behavior with a persistent corner spin mode the extraordinary class.

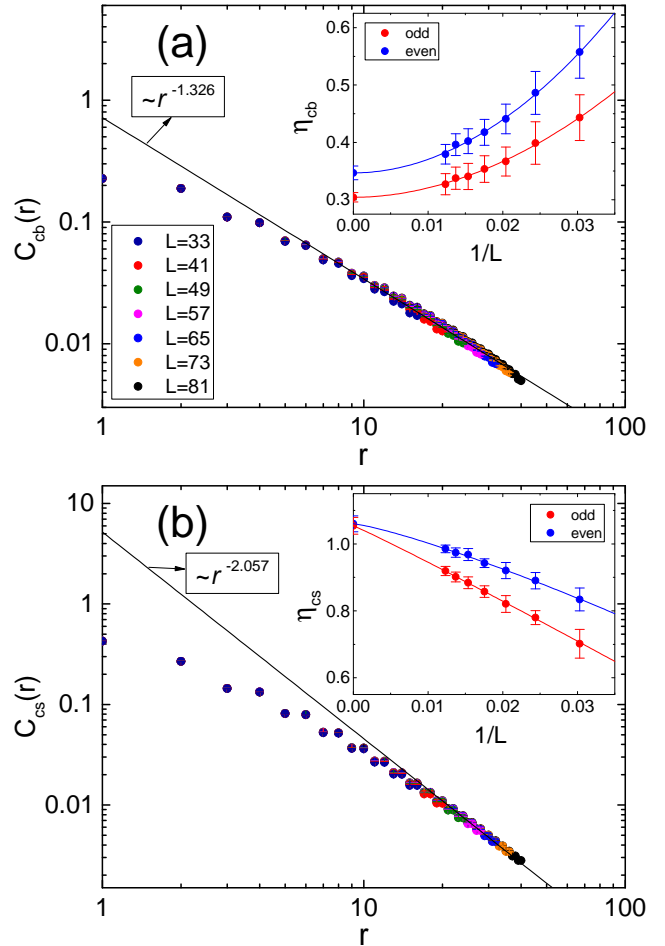


FIG. 4. Spatial correlation functions (a) $C_{cb}(r)$ and (b) $C_{cs}(r)$ of the dangling corner spin. The black lines are the reference for the power-law decay with the extrapolated critical exponents, $\eta_{cb} = 0.33(3)$ and $\eta_{cs} = 1.06(3)$. Insets: the finite-size scaling of the critical exponents η_{cb} and η_{cs} with Eq. (12).

This is quite surprising as we may expect that the spin-1/2 mode would be screened by the critical bulk state like the Kondo singlet formed a magnetic impurity immersed in a metal.

The spatial correlations $C_{cb}(r)$ and $C_{cs}(r)$ show a simple power-law scaling form. With the finite-size scaling analysis sketched in Sec. II, we find $\eta_{cb}^e = 0.347(11)$, $\eta_{cb}^o = 0.304(9)$, and $\eta_{cs}^e = 1.06(3)$, $\eta_{cs}^o = 1.05(3)$. Our final estimate of these exponents are

$$\eta_{cb} = 0.33(3), \quad \eta_{cs} = 1.06(3). \quad (21)$$

The scaling relations in Eqs. (10) and (11) are respected within error bars, thus our estimate of the scaling dimension of the corner spin operator is

$$\Delta_c = 0.841(6). \quad (22)$$

The free spin-1/2 corner mode can be described by the

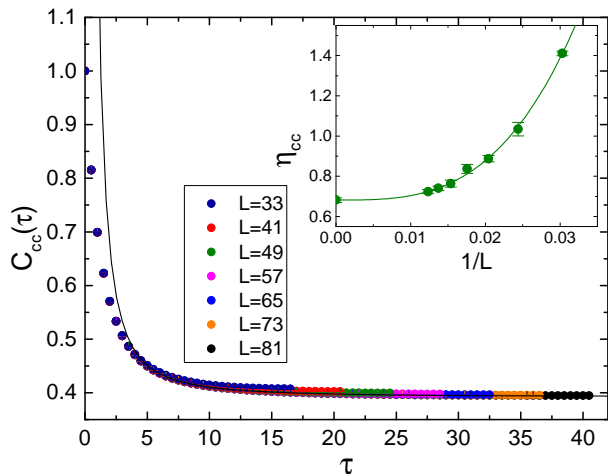


FIG. 5. Imaginary-time correlation function $C_{cc}(\tau)$ of the dangling corner spin, which does not decay to zero, indicating a persistent degenerate spin mode. Inset: the finite-size scaling of the critical exponent η_{cc} with Eq. (12).

Wess-Zumino-Witten term⁵⁰,

$$S[\hat{n}(\tau)] = \int d\tau \int_0^1 du (\hat{n}(\tau, u) \cdot (\partial_\tau \hat{n}(\tau, u) \times \partial_u \hat{n}(\tau, u))), \quad (23)$$

in which the unit vector $\hat{n}(\tau)$ represents the direction of the corner spin state, which is lifted to a continuous field $\hat{n}(\tau, u)$ over the imaginary time τ and an auxiliary parameter $u \in [0, 1]$. The lifting is an arbitrary continuous mapping satisfying

$$\hat{n}(\tau, u = 0) = (0, 0, 1), \quad \hat{n}(\tau, u = 1) = \hat{n}(\tau). \quad (24)$$

The scaling dimension of the unit vector $[\hat{n}] = 0$. The coupling of the corner spin to the bulk is captured by

$$S_c = g \int d\tau (\hat{n}(\tau) \cdot \vec{\phi}(\tau)), \quad (25)$$

in which $\vec{\phi}(\tau)$ is the antiferromagnetic order parameter at the corner of the bulk state with an ordinary corner criticality. The scaling dimension of the ordinary corner spin $[\vec{\phi}] = 1.67(2)$. Therefore, a simple dimension counting gives the scaling dimension of the coupling constant $[g] = -0.67(2) < 0$, thus the corner-bulk coupling is irrelevant. This might explain the persistent corner mode at the bulk QCP. However, it cannot explain the difference of the corner critical exponents from the ordinary class.

IV. CONCLUSION

To summarize, we have studied the corner critical behavior at the QCP of a plaquette Heisenberg model with extensive quantum Monte Carlo simulations. We find that the two corners with or without a dangling spin show different critical exponents, thus belong to different universality classes. In particular, the degenerate spin mode at the dangling corner, which is a hallmark of the HOSPT state in the disorder phase, persists at the bulk QCP despite its coupling to the critical spin fluctuations. This shows the unexpected robustness of the degenerate corner mode of the HOSPT state.

ACKNOWLEDGMENTS

We thank Xue-Feng Zhang for helpful discussion. This work is supported by the National Key R&D Program of China (2018YFA0305800), the National Natural Science Foundation of China (11804337, 12047564 and 12174387), the Strategic Priority Research Program of CAS (XDB28000000), the Fundamental Research Funds for the Central Universities under Grant No. 2020CDJQY-Z003 and the CAS Youth Innovation Promotion Association.

* xiongzjsysu@hotmail.com

† longzhang@ucas.ac.cn

¹ J. Cardy, *Scaling and Renormalization in Statistical Physics* (Cambridge University Press, Cambridge, 1996).

² T. Senthil, A. Vishwanath, L. Balents, S. Sachdev, and M. P. A. Fisher, *Science* **303**, 1490 (2004).

³ T. Senthil, L. Balents, S. Sachdev, A. Vishwanath, and M. P. A. Fisher, *Phys. Rev. B* **70**, 144407 (2004).

⁴ F. D. M. Haldane, *Phys. Rev. Lett.* **61**, 1029 (1988).

⁵ A. Tanaka and X. Hu, *Phys. Rev. Lett.* **95**, 036402 (2005).

⁶ T. Senthil and M. P. A. Fisher, *Phys. Rev. B* **74**, 064405 (2006).

⁷ K. Binder, in *Phase Transitions and Critical Phenomena*, Vol. 8, edited by C. Domb and J. L. Lebowitz (Academic Press, London, England, 1983).

⁸ H. W. Diehl, in *Phase Transitions and Critical Phenomena*, Vol. 10, edited by C. Domb and J. L. Lebowitz (Academic Press, London, 1986).

⁹ M. Cheng and H.-H. Tu, *Phys. Rev. B* **84**, 094503 (2011).

¹⁰ L. Fidkowski, R. M. Lutchyn, C. Nayak, and M. P. A. Fisher, *Phys. Rev. B* **84**, 195436 (2011).

¹¹ J. D. Sau, B. I. Halperin, K. Flensberg, and S. Das Sarma, *Phys. Rev. B* **84**, 144509 (2011).

¹² T. Grover and A. Vishwanath, arXiv:1206.1332.

¹³ L. Zhang and F. Wang, *Phys. Rev. Lett.* **118**, 087201 (2017).

¹⁴ C. Ding, L. Zhang, and W. Guo, *Phys. Rev. Lett.* **120**, 235701 (2018).

¹⁵ L. Weber, F. Parisen Toldin, and S. Wessel, *Phys. Rev. B* **98**, 140403 (2018).

- ¹⁶ L. Weber and S. Wessel, Phys. Rev. B **100**, 054437 (2019).
- ¹⁷ W. Zhu, C. Ding, L. Zhang, and W. Guo, Phys. Rev. B **103**, 024412 (2021).
- ¹⁸ C. Ding, W. Zhu, W. Guo, and L. Zhang, arXiv:2110.04762.
- ¹⁹ F. Parisen Toldin, Phys. Rev. Lett. **126**, 135701 (2021).
- ²⁰ M. Hu, Y. Deng, and J.-P. Lv, Phys. Rev. Lett. **127**, 120603 (2021).
- ²¹ F. Parisen Toldin and M. A. Metlitski, arXiv:2111.03613.
- ²² C.-M. Jian, Y. Xu, X.-C. Wu, and C. Xu, SciPost Phys. **10**, 033 (2021).
- ²³ M. A. Metlitski, arXiv:2009.05119.
- ²⁴ L. Weber and S. Wessel, Phys. Rev. B **103**, L020406 (2021).
- ²⁵ W. Zhu, C. Ding, L. Zhang, and W. Guo, arXiv:2111.12336.
- ²⁶ X.-J. Yu, R.-Z. Huang, H.-H. Song, L. Xu, C. Ding, and L. Zhang, arXiv:2111.10945.
- ²⁷ W. A. Benalcazar, B. A. Bernevig, and T. L. Hughes, Science **357**, 61 (2017).
- ²⁸ W. A. Benalcazar, B. A. Bernevig, and T. L. Hughes, Phys. Rev. B **96**, 245115 (2017).
- ²⁹ Z. Song, Z. Fang, and C. Fang, Phys. Rev. Lett. **119**, 246402 (2017).
- ³⁰ J. Langbehn, Y. Peng, L. Trifunovic, F. von Oppen, and P. W. Brouwer, Phys. Rev. Lett. **119**, 246401 (2017).
- ³¹ F. Schindler, A. M. Cook, M. G. Vergniory, Z. Wang, S. S. P. Parkin, B. A. Bernevig, and T. Neupert, Sci. Adv. **4**, eaat0346 (2018).
- ³² L. Trifunovic and P. W. Brouwer, Phys. Rev. X **9**, 011012 (2019).
- ³³ Y. Wang, M. Lin, and T. L. Hughes, Phys. Rev. B **98**, 165144 (2018).
- ³⁴ Y. You, T. Devakul, F. J. Burnell, and T. Neupert, Phys. Rev. B **98**, 235102 (2018).
- ³⁵ O. Dubinkin and T. L. Hughes, Phys. Rev. B **99**, 235132 (2019).
- ³⁶ C. Peng, L. Zhang, and Z.-Y. Lu, Phys. Rev. B **104**, 075112 (2021).
- ³⁷ S. Wenzel, L. Bogacz, and W. Janke, Phys. Rev. Lett. **101**, 127202 (2008).
- ³⁸ S. Wenzel and W. Janke, Phys. Rev. B **79**, 014410 (2009).
- ³⁹ X. Ran, N. Ma, and D.-X. Yao, Phys. Rev. B **99**, 174434 (2019).
- ⁴⁰ Y. Xu, Z. Xiong, H.-Q. Wu, and D.-X. Yao, Phys. Rev. B **99**, 085112 (2019).
- ⁴¹ A. W. Sandvik, J. Phys. A **25**, 3667 (1992).
- ⁴² A. W. Sandvik, Phys. Rev. B **59**, R14157 (1999).
- ⁴³ A. Dorneich and M. Troyer, Phys. Rev. E **64**, 066701 (2001).
- ⁴⁴ O. F. Syljuåsen and A. W. Sandvik, Phys. Rev. E **66**, 046701 (2002).
- ⁴⁵ F. Kos, D. Poland, D. Simmons-Duffin, and A. Vichi, J. High Energy Phys. **2016**, 36 (2016).
- ⁴⁶ D. Poland, S. Rychkov, and A. Vichi, Rev. Mod. Phys. **91**, 015002 (2019).
- ⁴⁷ H. W. Diehl and M. Shpot, Phys. Rev. Lett. **73**, 3431 (1994).
- ⁴⁸ H. Diehl and M. Shpot, Nucl. Phys. B **528**, 595 (1998).
- ⁴⁹ F. Gliozzi, P. Liendo, M. Meineri, and A. Rago, J. High Energy Phys. **2015**, 36 (2015).
- ⁵⁰ A. Auerbach, *Interacting electrons and quantum magnetism* (Springer, 1994).